JOURNAL OF GEOPHYSICAL RESEARCH, VOL. 101, NO. B5, PAGES 11,275–11,290, MAY 10, 1996

Mapping the descent of Indian and Eurasian plates beneath the Tibetan Plateau from gravity anomalies

Yu Jin and Marcia K. McNutt

Department of Earth, Atmospheric, and Planetary Sciences, Massachusetts Institute of Technology Cambridge

Yong-sheng Zhu

Department of Marine Geology, Ocean University of Qingdao, Qingdao, China

Abstract. The collision of India with Asia has produced a complicated continental-continental plate boundary involving folding and faulting of variable trends and styles within and along the margins of the Tibetan Plateau. Numerous lines of evidence, including the development of two scales of folding in Tibet, suggest that the lowermost crust is behaving in a ductile fashion. This weak lower crust might then decouple the fundamental plate tectonic motions in the uppermost mantle from the complex pattern of surface faulting. In this study, we use Bouguer gravity anomalies to map out the geometry of Indian and Eurasian plate interactions in the mantle beneath the plateau based on both the inferred geometry of the Moho and lateral variations in lithospheric strength determined from mechanical modeling. In our preferred model, the lithosphere beneath Tibet consists of two distinct units: (1) the underthrust (to the north) Indian plate, which sutures with the Eurasian plate in the upper mantle below the Yarlung-Zangpo Suture or the Gangdese igneous belt, 200-400 km north of the Main Boundary Thrust, and (2) the underthrust (to the south) Eurasian plate. A subducting slab of Indian upper mantle extends about 200 km into the asthenosphere north from the mantle suture and exerts a bending moment of about 3.5×10^{17} N on the Indian plate. Thus the mantle lithosphere appears to be behaving in the simple fashion of converging oceanic plates, while the more buoyant continental crust deforms under high gravitational potential in a complex pattern controlled by its lateral and vertical strength heterogeneity.

Introduction

Understanding plate tectonic motion is relatively simple over the two-thirds of the Earth's surface covered by oceans: drift of the oceanic crust at the surface of the plate is tightly coupled to that of the mantle portion of plate. However, on the continents, surface faults often do not have a simple relationship with the lithospheric mantle on account of heterogeneity in deformational properties of continental rocks [*Burchfiel et al*, 1989; *Molnar and Lyon-Caen*, 1989; *Yin et al.*, 1994; *Masek et al.*, 1994; *McNamara et al.*, 1995]. Lack of correspondence between the surface and mantle plate boundaries might be particularly severe in cases where the crustal thickness is so great or heat flow is so high that the lowermost continental crust behaves in a ductile fashion, acting to partially decouple the motions in the mantle from net motion accomplished by surface faulting. In such cases it is necessary to rely on geophysical techniques, such as mapping earthquake hypocenters in the mantle, lateral variations in seismic properties, heat flow anomalies, or gravity anomalies, in order to reveal the plate interactions at depth.

Paper number 96JB00531.
0148-0227/96/96JB-00531$09.00

If mantle lithosphere and crust are decoupled as stated above [*Willett and Beaumont*, 1994; *Royden and Burchfiel*, 1995; *Yin et al.*, 1994], the mantle portion of the continent-continent plate boundary where the Indian plate is colliding with the Eurasian plate may be buried somewhere far beneath the Tibetan Plateau, the highest land mass on Earth. Plate reconstructions and the polarity of paired metamorphic belts imply that the initial collision between the Indian subcontinent and Asia involved north-dipping subduction of Tethyan seafloor beneath the southern margin of Eurasia prior to about 50 million years ago [*Boulin*, 1981; *Sinha-Roy*, 1982]. Maps of the surface geology present a very complicated scenario for how that collision is being accommodated at present, at least in terms of crustal deformation. The current locus of thrusting occurs mainly along the Main Boundary Thrust (MBT) at the southern foot of the Himalayas (Figure 1), but this is clearly absorbing shortening within Indian crust since the geologic boundary between rocks of Indian versus Asian affinity occurs farther north at the Yarlung-Zangpo suture zone, which has been severely modified by north and south dipping crustal thrust systems [*Yin et al.*, 1994]. To complicate matters even further, the predominant pattern of contemporary deformation within the Tibetan Plateau consists of roughly east-west-trending strike-slip faulting [*Molnar and Tapponnier*, 1975; *Tapponnier et al.*, 1982; *Burchfiel et al.*, 1989], with even some east-west extension occurring in the high Himalaya [*Armijo et al.*, 1986; *Dewey et al.*, 1988; *Pan and Kidd*, 1992;

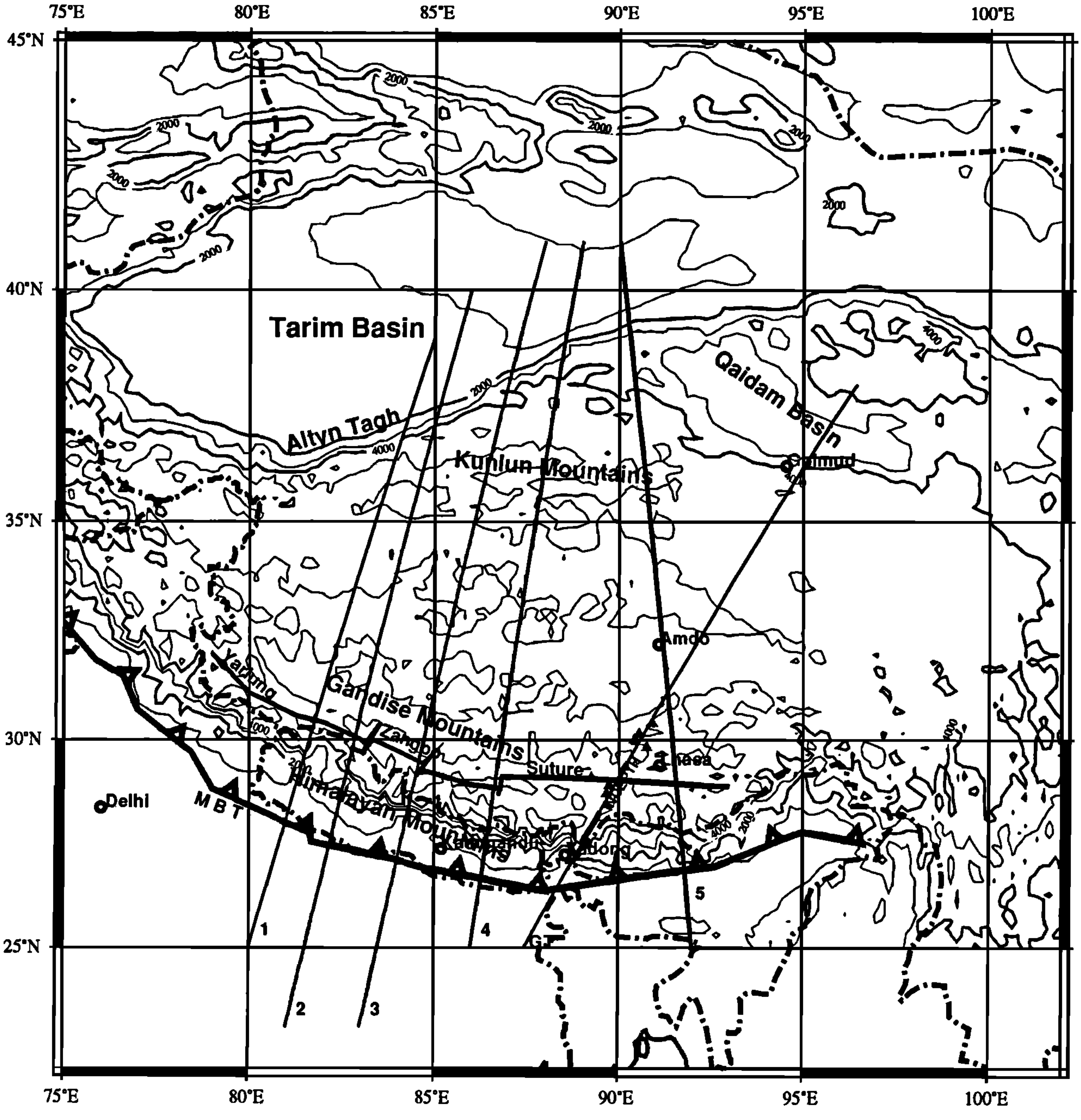

Figure 1. Location map for the Tibetan Plateau. Numbered lines are the locations of the profiles modeled in this paper. Dash-dotted lines are political boundaries. The background contour is topography in meters. MBT is the Main Boundary Thrust. Profile GT is along the Geotransect 3. The short, heavy line north of Yadong shows the location of the INDEPTH seismic reflection profile [*Zhao et al.*, 1993]. The triangles to the north of INDEPTH are the locations of a temporary deployment of broadband seismic stations.

Masek et al., 1994]. More north-south shortening in response to the collision is accommodated at the northern edge of the plateau, where a flexural foredeep has developed along the southern edge of the Tarim Basin [*Avouac and Peltzer*, 1993], and again even farther north within the Tien Shan, a Paleozoic fold belt reactivated by folding and faulting in the Tertiary [*Avouac et al.*, 1993].

The question we address here is whether the complex surface pattern of deformation reflects deformation in the mantle as well, or whether plate boundaries at depth are fundamentally very simple, just as they are in the ocean basins. Theoretical models for the uplift of the Tibetan Plateau have made two very different assumptions concerning this point. For example, the viscous sheet models of *England and McKenzie* [1982] implicitly assume a single plate, with the mantle thickening and deforming in concert with the overlying crust. On the other hand, the numerical simulations of *Willett and Beaumont* [1994] assume that a weak lower crust partially decouples the upper crust from the mantle, which is modeled as the Eurasian plate underthrusting the Indian plate beneath the northern edge

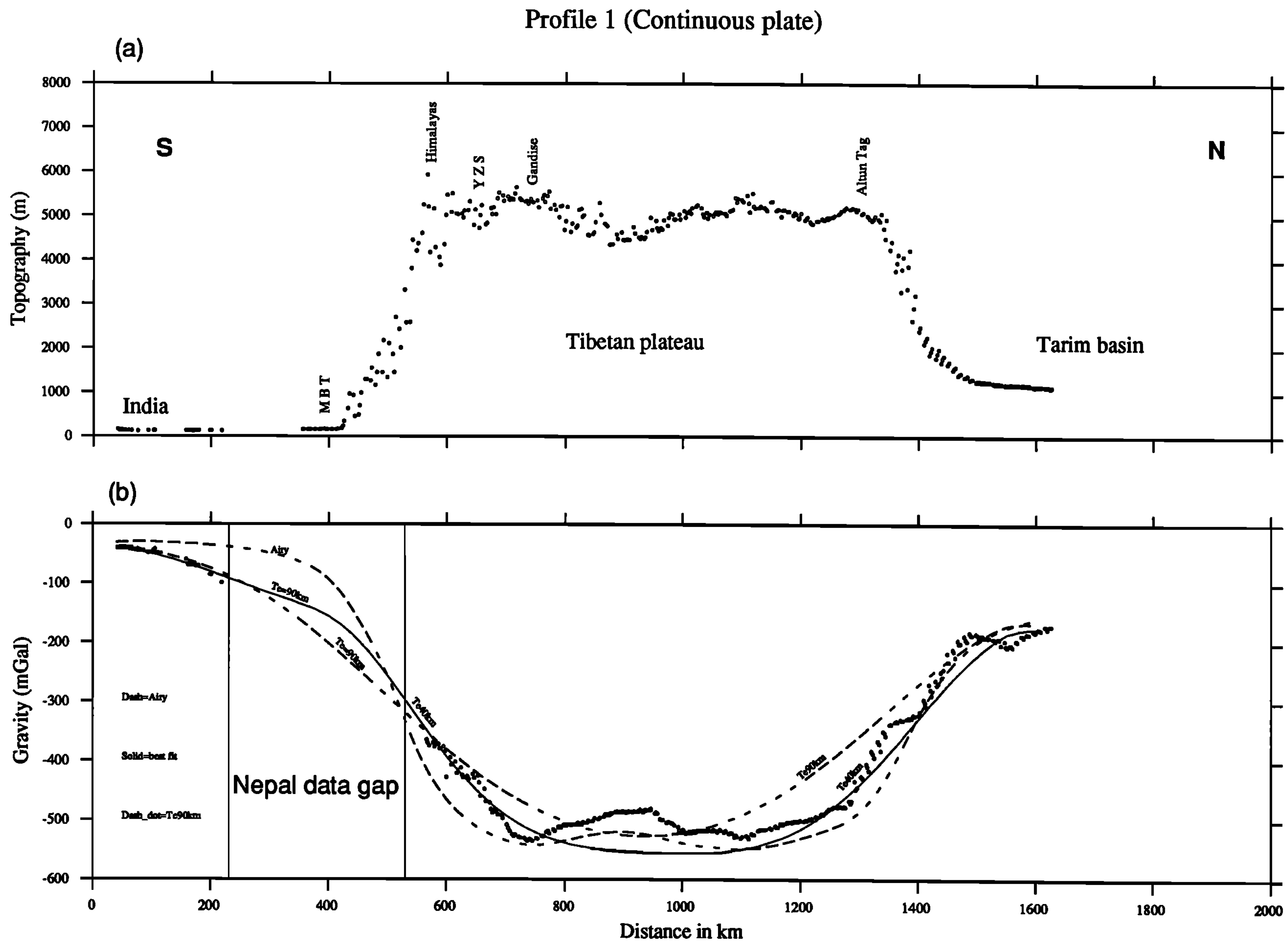

Figure 2. Fit of simple continuous plate models to Bouguer gravity data along profile 1. (a) Topography. (b) Bouguer gravity and predicted Bouguer gravity for Airy isostasy, a constant rigidity elastic plate with T_e=90 km, and a variable rigidity model for a continuous plate. The Nepal data gap is located at the large transition zone of gravity and topography.

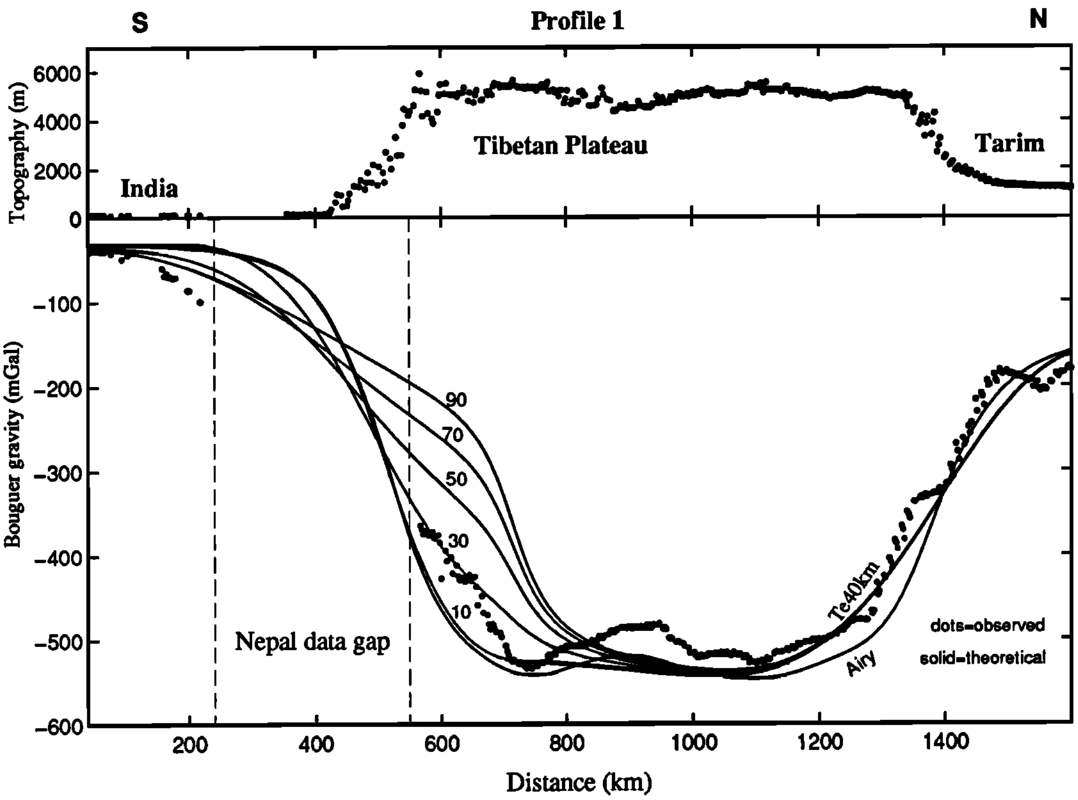

Figure 3. Topography and Bouguer gravity along profile 1, showing model fits for a two-plate system with several different values for the constant elastic plate thickness for the Indian plate on the south. The Eurasian plate to the north is assumed to have an elastic thickness of 40 km. The Bouguer gravity predicted by the Airy model is shown for reference. The observed topography is the only load on the plates.

of the plateau. This scenario requires a reversal in subduction polarity since the time of subduction of Tethyan seafloor and predicts largely independent strain patterns in the crust versus the mantle. In this study we use Bouguer gravity and topographic data to constrain the geometry of the plates beneath the Tibetan Plateau.

The Data

The area for which we obtained Bouguer gravity and topography data is shown in Figure 1. Most of the area is in the People's Republic of China, bounded by India in the south and by the former Soviet Union in the northwestern corner of the map. The data in China were compiled by Ocean University of Qingdao, People's Republic of China. The original point gravity measurements were based on the Potsdam standard within the geographical reference of the Beijing Coordinate System and the Yellow Sea Elevation System. Data were reduced using the Helmert normal gravity formula for gravity on the spheroid and converted to free air anomalies. The Bouguer gravity field was calculated using a topographic density of 2670 kg/m^3, and terrain corrections were applied out to a distance of 166.7 km [*Sun*, 1989]. Through a scientific collaboration agreement between the Ocean University of Qingdao and the Massachusetts Institute of Technology, the gravity and topography data were interpolated for us onto a 5 arc min × 5 arc min grid. Although the original point measurements were fairly evenly distributed over the plateau, the lower limit on the wavelengths resolved is closer to 10 arc min than 5 arc min, except in a few well-sampled areas. The cumulative error in the Bouguer gravity field is estimated to be 1.5 mGal [*Sun*, 1989], including errors in elevation but not uncertainty in the Bouguer reduction density. The validity of the topographic data was verified by E. Fielding at Cornell University by comparing our values over a 2°x2° area with an independent, even higher-resolution, digital elevation model [*Fielding et al.*, 1994]. Although there is a small discrepancy in the registration of the two topographic data sets, the average differences are less than 10 m.

The data on the Indian side are from the Lamont Geobase, which includes land gravity measurements assembled from various sources by G. Karner and others at Lamont-Doherty Earth Observatory of Columbia University [*Watts et al.*, 1985]. The lack of gravity constraints from Nepal (about 200 km) leaves an unfortunate gap in the gravity signal from the Indian plate descending beneath the Himalaya in the region where a major change in gravity gradient occurs. The exact location of the change in gradient therefore remains unconstrained (profiles 1-5 in Figures 8-12). The gravity data in the former Soviet Union are described by *Kogan and McNutt* [1993].

Modeling Strategy

Bouguer gravity anomalies reflect lateral variations in density at depth. The largest vertical density discontinuity near but beneath Earth's surface occurs at the Moho. In order

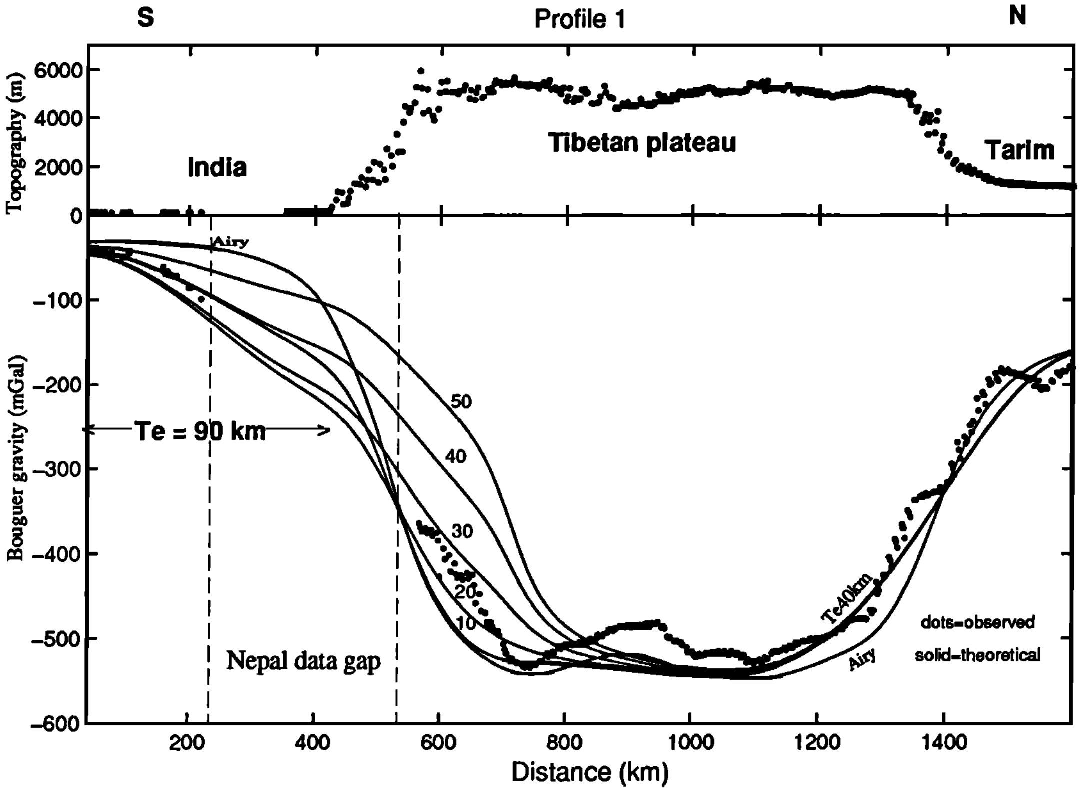

Figure 4. Elastic plate models as in Figure 3, except that the Indian plate is allowed to weaken beneath the Himalaya. Beneath the Ganges Basin, the elastic plate thickness for India is fixed at 90 km. The observed topography is the only load on the plates.

to maintain isostatically the elevation of the high and broad Tibetan Plateau, the thickness of the Tibetan crust is approximately doubled compared to that of the Ganges and Tarim basins south and north of the plateau, respectively. This large variation in Moho depth contributes most of the signal in the Bouguer gravity anomaly. In our previous examination of the gravity field over Tibet [*Jin et al.*, 1994], we inferred that the source of the Bouguer gravity anomaly at wavelengths greater than 230 km is located at the presumed depth of the Moho or deeper, with the shorter-wavelength signal arising from folding and faulting of shallower density discontinuities within the upper crust. The short-wavelength (< 230 km) part of the gravity signal suggests that the Tibetan lithosphere is rheologically layered, consisting of mechanically competent upper crustal and mantle layers separated by a weak low-viscosity zone in the lower crust. The longer-wavelength (> 230 km) portion of the signal that originates at or below the Moho contains approximately 95% of the power in the total signal. Therefore in what follows we model the longer-wavelength Bouguer gravity signal as arising from deformation of the upper mantle in response to the weight of the plateau and plate collision.

We considered fits of flexural models to six profiles across the plateau (Figure 1). Profiles 1-5 are perpendicular to the Main Boundary Thrust (MBT in Figure 1) and profile GT is along Geotransect 3 [*Wu et al.*, 1991] to compare with the results from the INDEPTH seismic reflection project [*Zhao et al.*, 1993]. Because of the lack of prior constraints on the structure of the upper mantle beneath Tibet, we had to allow for a considerable latitude in possible plate models. For example, we examined the best fitting models assuming either one continuous plate beneath Tibet or up to three separate plates. The elastic plate thickness (T_e) of the plate or plates was allowed to vary laterally, and we had to consider the possibility of lateral compression on the system. Theoretical deflection of the elastic plate or plates was calculated using the two-dimensional finite difference method of *Sheffels and McNutt* [1986] for pairs of variable-rigidity elastic plates subjected to vertical and horizontal loads, and the corresponding gravity was computed using *Okabe*'s [1979] formula. The surface load was assigned a uniform density of 2670 kg/m^3, except in the Tarim Basin just north of the plateau where we allowed for a 1-km thickness of sand with density 2100 kg/m^3 and 6 km of sediments with an average density of 2500 kg/m^3 [*Teng et al.*, 1991].

Results

Although interpretation of gravity data is always nonunique, the following features became apparent as we examined fits to the data along the six profiles under various modeling assumptions. These features will be illustrated only on profile 1, although the conclusions are generally valid for all cross sections.

1. No continuous plate of uniform or variable rigidity comes close to fitting the gravity along the complete profiles from the Indian plate north across the plateau to the Tarim Basin. Figure 2 examines the fit to the gravity data along profile 1 for several simple models: Airy isostasy (T_e=0 km), an elastic plate (T_e=90 km), and the best fitting continuous

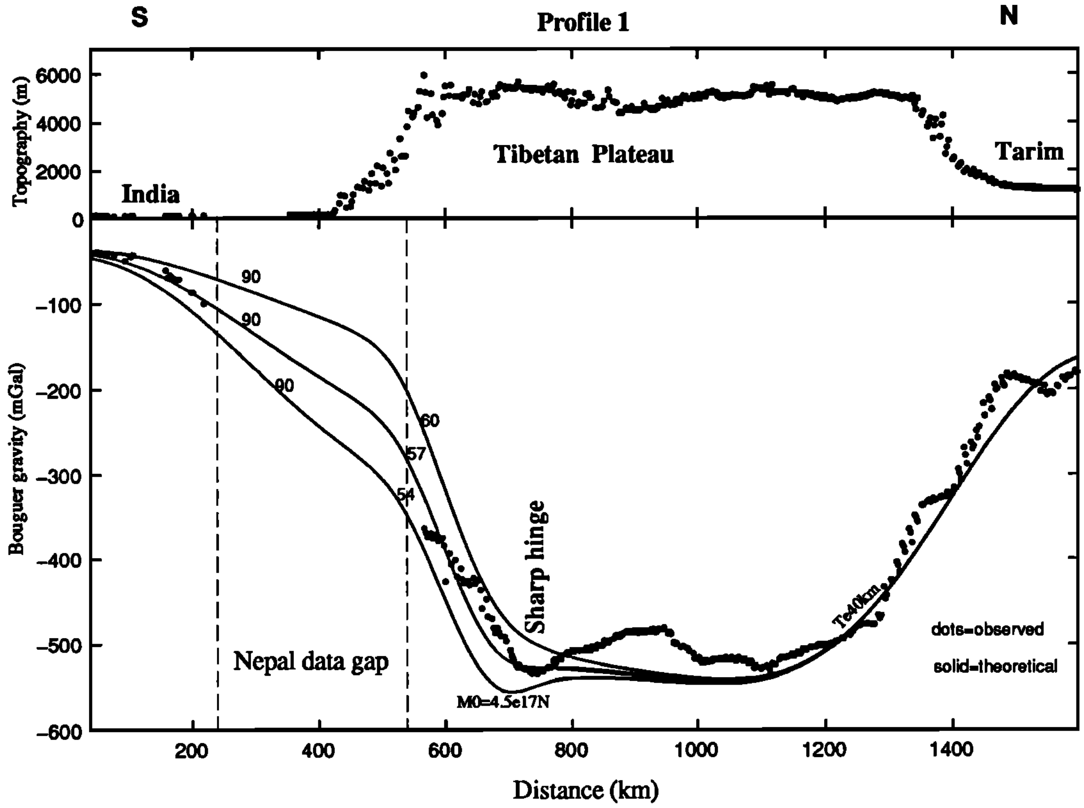

Figure 5. Elastic plate models as in Figure 4, except that a terminal bending moment M=4.5 x 10^{17} N is applied to the Indian plate at the mantle suture between the Indian and Eurasian plates, assumed to correspond to the sharp hinge zone as marked.

elastic plate with variable rigidity. Even the best continuous plate model produces large, systematic misfits to the data (root-mean-square misfit of 31 mGal out of a total signal of 422 mGal), and is only a marginal improvement over the Airy model (misfit=37 mGal).

2. Successful models all required a high-rigidity Indian plate on the south (elastic plate thickness T_e=90 km beneath the Ganges Basin) and a moderately rigid (T_e=40-45 km) Eurasian plate (consisting of lithosphere from the Tarim Basin and Tibet) on the north (Figure 3) in order to match the dip of the underthrust Indian plate from the south and the dip caused by regional compensation from the low Tarim Basin to the high Tibetan Plateau from the north. These values are quite consistent with those determined previously using the same data for the Indian plate [*Karner and Watts*, 1983; *Lyon-Caen and Molnar*, 1983; *Royden*, 1993] and a meager set of 16 pendulum gravity measurements [*Armboldt*, 1948] for the Tarim Basin [*Lyon-Caen and Molnar*, 1984].

3. Fits to the Bouguer gravity data along all of the profiles were substantially improved when the Indian plate was allowed to weaken while passing beneath the high Himalaya (Figure 4). The exact location of the change in rigidity is difficult to pin down on some profiles because of the absence of gravity data from Nepal, but the fact that the inferred trend of the Bouguer gravity beneath Tibet from the Chinese data lines up with that from the Indian side suggests that we are seeing a change in rigidity within one plate rather than the end of the Indian plate, which must lie well north of Nepal. The descent of the Asian plate can be traced continuously, and more modest weakening is also observed (T_e drops to 30 or 35 km).

4. The sharp hinge at about 300 km from the MBT cannot be matched with any continuous plate models; we interpret the hinge zone as the mantle suture between the Indian and Asian plates. Simply breaking the elastic plate at this hinge is still not sufficient to match the gravity data for the Indian plate, however, unless we add a bending moment of about 4.5×10^{17} N to the end of the Indian plate (Figure 5).

5. The positive upwarp of the observed Bouguer gravity at the center of the plateau for a distance of typically 400 km (Figure 5) is inconsistent with elastic models of any rigidity subjected to vertical loads, bending moments, and/or horizontal compression. One possible explanation is to model the upwarp in the gravity field beneath Tibet as buckling of an elastic-plastic plate [e.g., *McAdoo and Sandwell*, 1985]. However, the overburden pressure at the depth of the Tibetan Moho is so large that in-plane forces exceeding 1.6 GPa (16 kbar) are required to produce an arch of the correct magnitude, even assuming complete failure of the elastic core of an elastic-plastic plate. Although we cannot rule out the possibility that large in-plane forces act on the mantle lithosphere beneath Tibet, it is unlikely that they are solely responsible for the gravity arch over the center of the plateau.

6. On the other hand, we obtain an excellent fit to the data (misfit of 20 mGal) if we assume that the source of the bending moment on the Indian plate discussed in feature 4 above is a

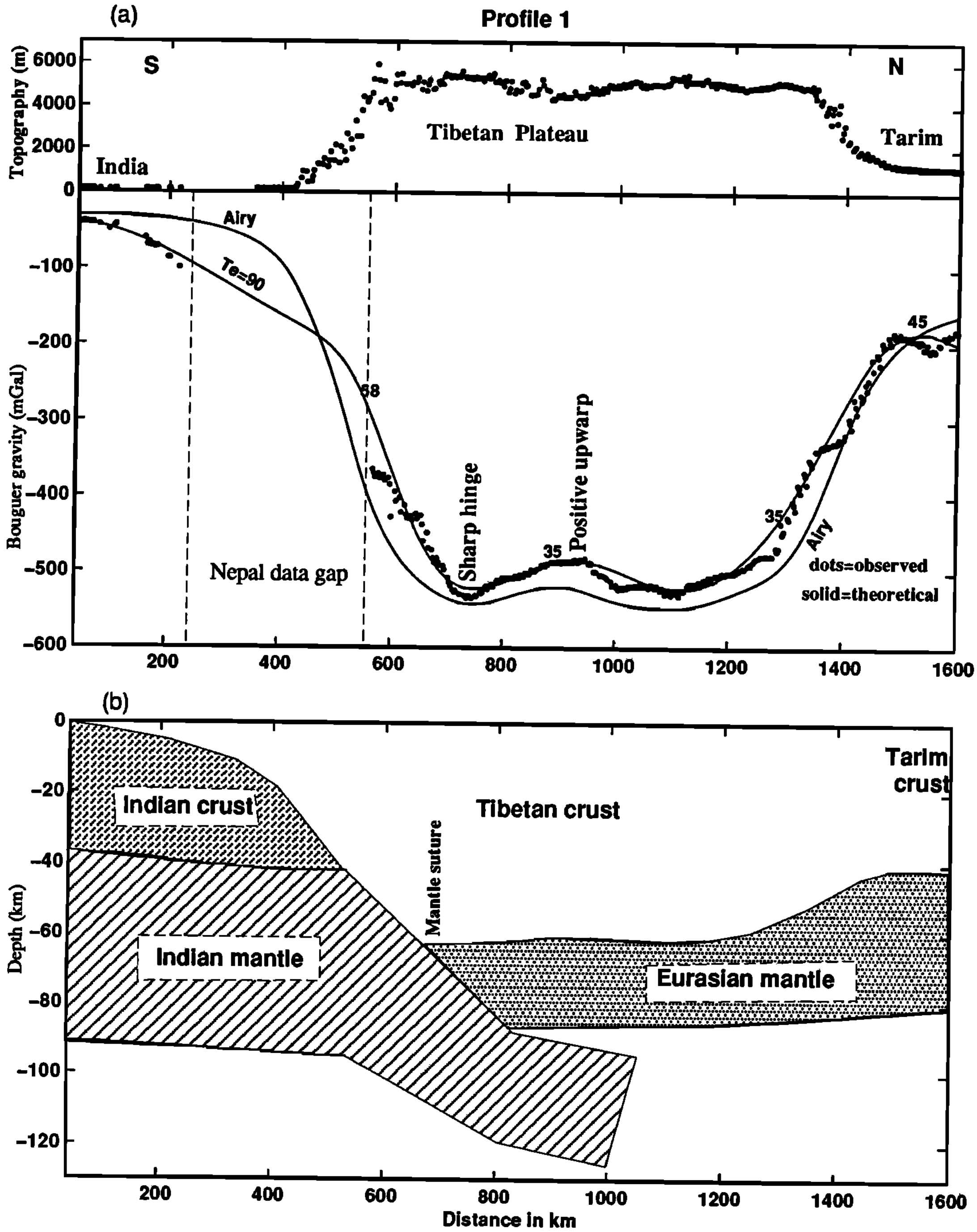

Figure 6. (a) Fit to the Bouguer gravity data along Profile 1 for a model in which the Indian plate has an initial elastic thickness of 90 km, which reduces to 58 km after it passes beneath the high Himalaya. The Eurasian plate begins with an elastic thickness of 45 km, which reduces to 35 km beneath the northern part of the plateau. The mantle suture lies at the hinge zone. The positive upwarp in the gravity data is caused by a slab of subducted Indian lithosphere underlying central Tibet which also supplies a bending moment to the Indian side of the plate system. The gravity prediction for Airy isostasy are shown for reference. (b) Crustal model corresponding to the gravity interpretation in (a). Because the fit to the Bouguer gravity data in (a) only depends on the product $\Delta\rho\ w$ where $\Delta\rho$ is the density contrast across the Moho and w is the Moho deflection, the absolute depth of the Moho is not uniquely determined by gravity modeling alone without some assumption of $\Delta\rho$. In this case, we chose $\Delta\rho$=400 kg/m^3 so that our Moho depths would agree with those derived from INDEPTH seismic data from southern Tibet [*Makovsky and Klemperer*, 1995. J. Ni, personal communication].

subducting slab with a density contrast of 100 kg/m^3 relative to the surrounding asthenosphere (Figure 6). Since 20 mGal is also the size of the gravity contribution from folding and faulting of the upper crust that we have not attempted to model here, we consider this model an acceptable fit to the gravity data. In this scenario the gravity arch is not reflecting Moho geometry but rather is reflecting the gravity effect of the slab below the Tibetan upper mantle.

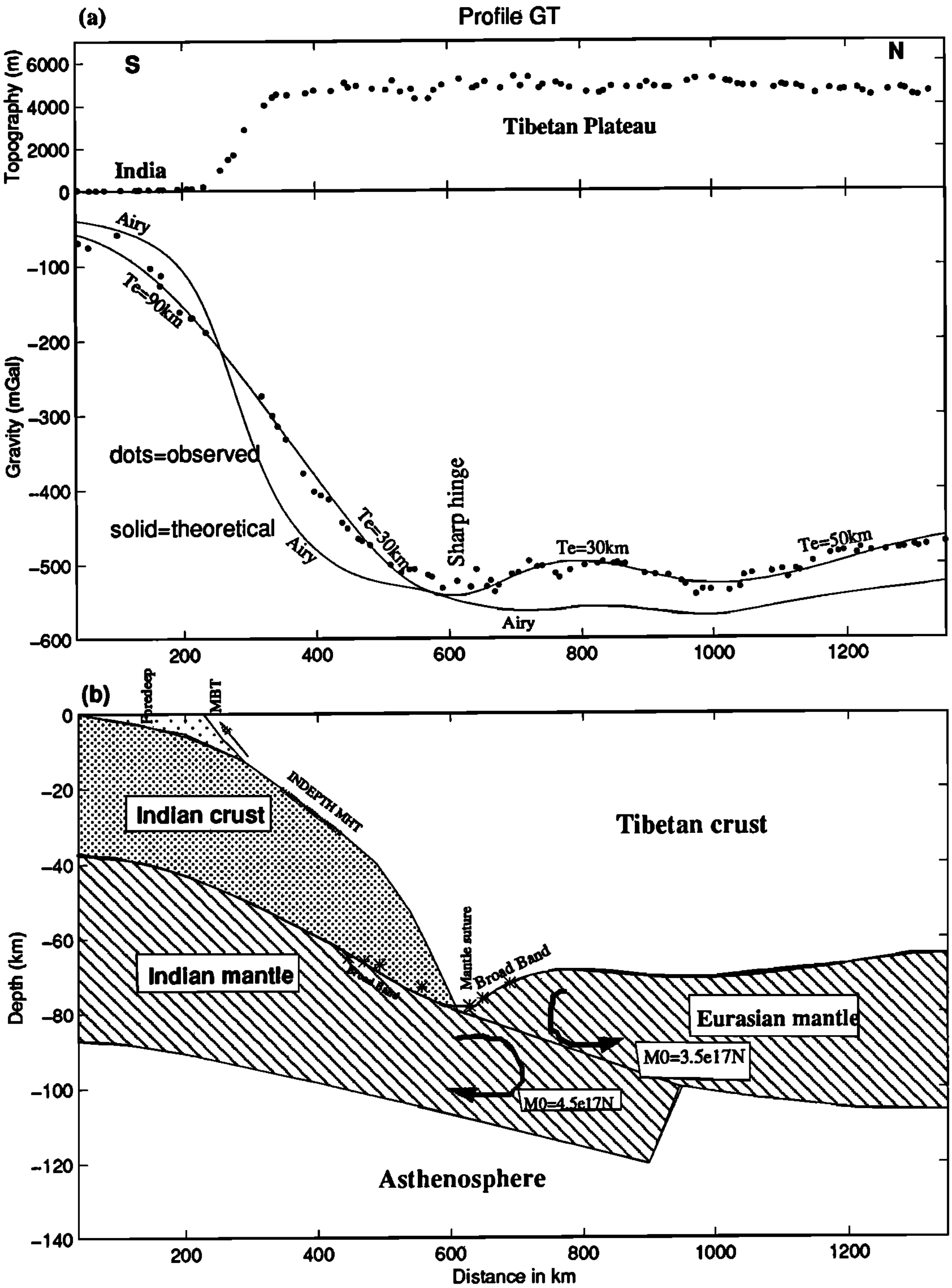

Figure 7. (a) Fit to the Bouguer gravity data along profile GT for a model in which the Indian plate has an initial elastic thickness of 90 km, which reduces to 30 km after it passes beneath the high Himalaya. The rigidity of the Eurasian plate is not well constrained on this profile, but elastic plate thicknesses between 30 and 50 km fit the data well. The mantle suture lies at the hinge zone. The Indian plate is subjected to a terminal bending moment of 4.5 x 10^{17} N by a slab of subducted material. The positive upwarp in the gravity data is caused by this subducted slab and by a moment of 3.5 x 10^{17} N applied to the Eurasian plate. This moment could be produced by 20-50 MPa of shear stress along the mantle suture. The gravity prediction for Airy isostasy is shown for reference. (b) Comparison of crustal model corresponding to the gravity fit from Figure 7a to INDEPTH seismic reflection data [*Makovsky and Klemperer*, 1996] and broadband seismic data (stars around the mantle suture) (J. Ni, personnal communication, 1995) along profile GT. The Indian foredeep basin and the Main Boundary Thrust (MBT) location are schematic. MHT is the Main Himalayan Thrust.

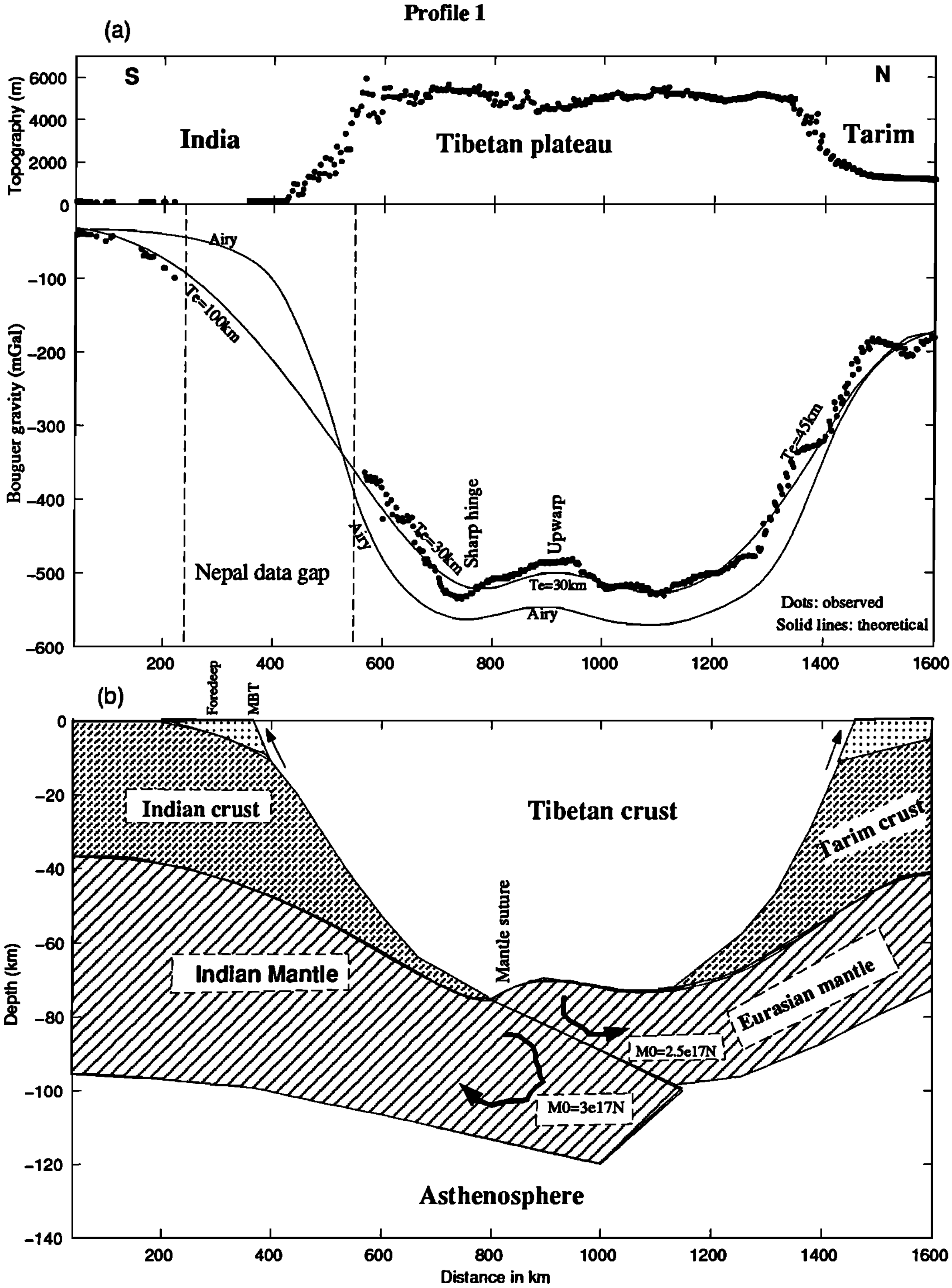

Figure 8. Same as Figure 7, except for data from profile 1. The best fitting elastic plate thicknesses and bending moments are as shown. The crustal thicknesses on both sides are derived from the lower limits of the mechanical thicknesses for both plates. The Indian foredeep and the Tarim sediments are schematic.

7. A slightly more complicated model (Figure 7) includes the gravitational effect of the subducted slab and the effect of 20-50 MPa of shear stress on the fault surface between the subducting Indian plate and the overriding Asian plate. Most of the upwarp in the observed Bouguer gravity still comes from the extra mass of the subducted Indian plate, but in comparison to the model described in feature 6, some relief on the Moho beneath Tibet is now produced by the bending moment generated by the shear stress on the fault. This model agrees well with Moho depths (Figure 7) acquired during the recent deployment of broadband seismometers associated with the INDEPTH II project (J. Ni, personal communication, 1995). Figures 8-12 show the fits to the gravity data of this preferred plate solution, including the mechanical and

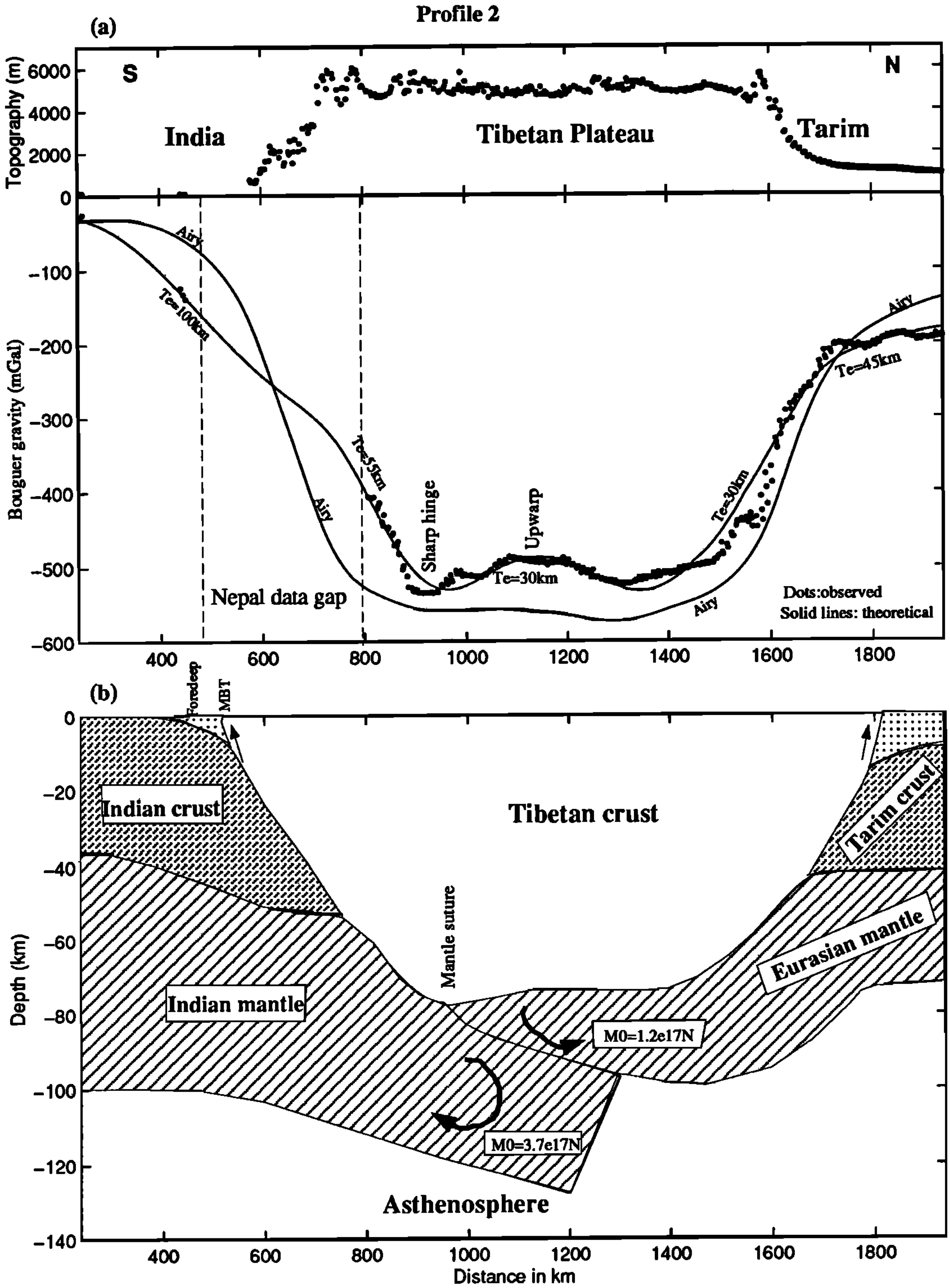

Figure 9. Same as Figure 8, but for profile 2.

gravitation effects of the subducting Indian plate, along the other five cross sections. The rms misfit of this subducting slab model is about 20 mGal, an improvement of nearly a factor of 2 over the Airy and continuous plate models.

Discussion

We can use other geological and geophysical information to test some features of our model derived from gravity. For example, the position of the Indian plate is constrained at least locally from INDEPTH deep seismic reflection data [*Zhao et al.*, 1993] coincident with our profile GT (Figure 7). The reflector depths [*Makovsky and Klemperer*, 1996] from the Main Himalayan Thrust (MHT) in INDEPTH correspond to the skinned top of the Indian plate in our model.

Another test of our model is whether the amount of underthrusting of the Indian plate provides sufficient convergence to create the topographic plateau. Along each

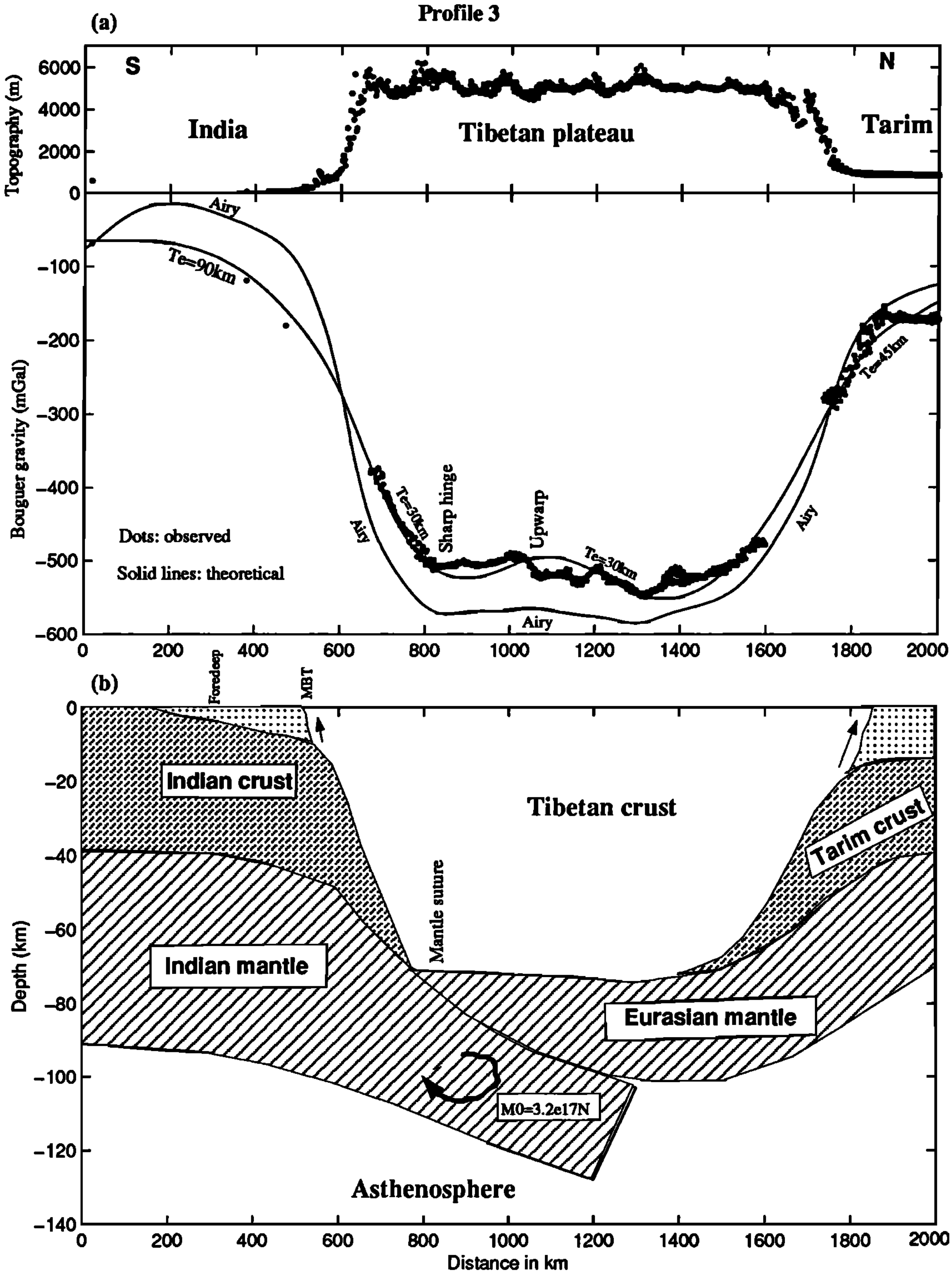

Figure 10. Same as Figure 8, but for profile 3.

profile we modeled, the subducting Indian plate extends 200-400 km north of the Yarlung-Zangpo Suture (YZS), or 500-700 km north of the MBT. If 40 km of crust is scraped off the Indian plate between the mantle suture and the apparent end of the slab (assuming this represents subducted continental lithosphere) as determined from gravity modeling, the Tibetan crust could be thickened from 40 to 60 km across a plateau 800 km wide. This simple calculation based on a series of two-dimensional profiles thus accounts for most, but perhaps not all, of the observed crustal thickening. Arc magmatism prior to continent-continent collision and obduction of oceanic sediments might also have contributed to crustal thickening. Note that according to our model, crustal thickening occurs by some sort of crustal injection within the lower crust, in the manner of *Zhao and Morgan* [1987], and thus does not predict any significant overthrusting of the Tarim Basin along the Altyn Tagh at the northern boundary of the plateau.

The best fit to the gravity data along all profiles assumes that the subducted part of the Indian plate north of the YZS lies nearly horizontally (inferred dips of 2° to 4°) beneath the

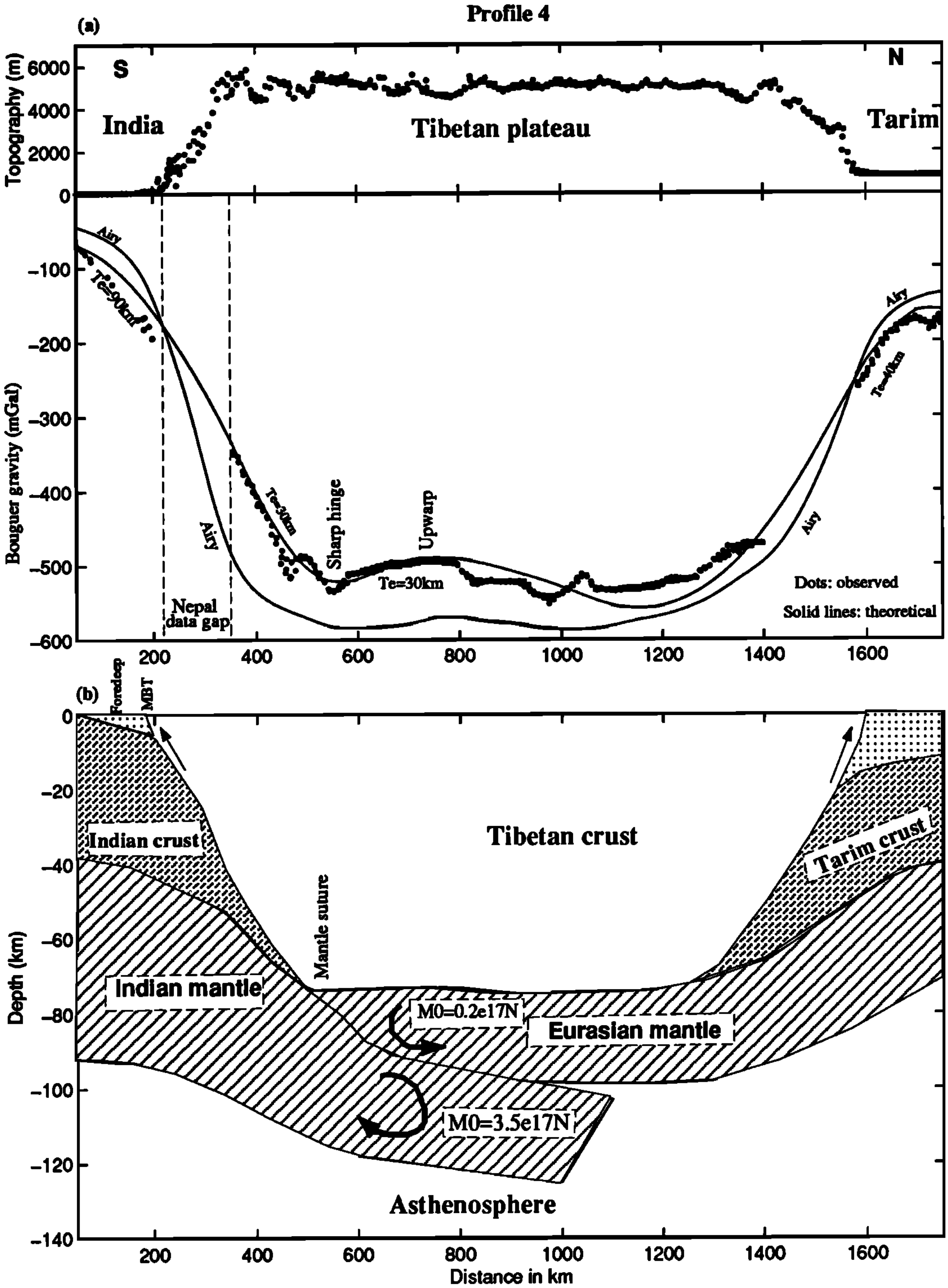

Figure 11. Same as Figure 8, but for profile 4.

Eurasian lithosphere, in effect, underplating it up to a point just north of the central part of the plateau (Figure 13). It is intriguing to note that the zone of inefficient S_n propagation identified by *Ni and Barazangi* [1983] and *Beghoul et al.* [1993] lies in the slabless window just north of the end of the subducted Indian plate according to our gravity model.

The most likely source of the shear stresses (mentioned in feature 7) on the lithospheric fault separating the Indian and Asian plates in our preferred model is lateral compression across this collision zone. Depending on the exact dip of the fault, average shear stresses of 20-50 MPa would correspond to lateral compression of 100 to 200 MPa (1 to 2 kbar) averaged over the thickness of the plate. Stresses of this magnitude may cause olivine-rich mantle minerals in the Eurasian upper mantle to line up in the E-W direction and produce the observed shear wave splitting beneath nothern Tibet [*McNamara et al.*, 1994]. Also, the only deep earthquake in the Harvard centroid moment tensor (CMT) catalogue is at the

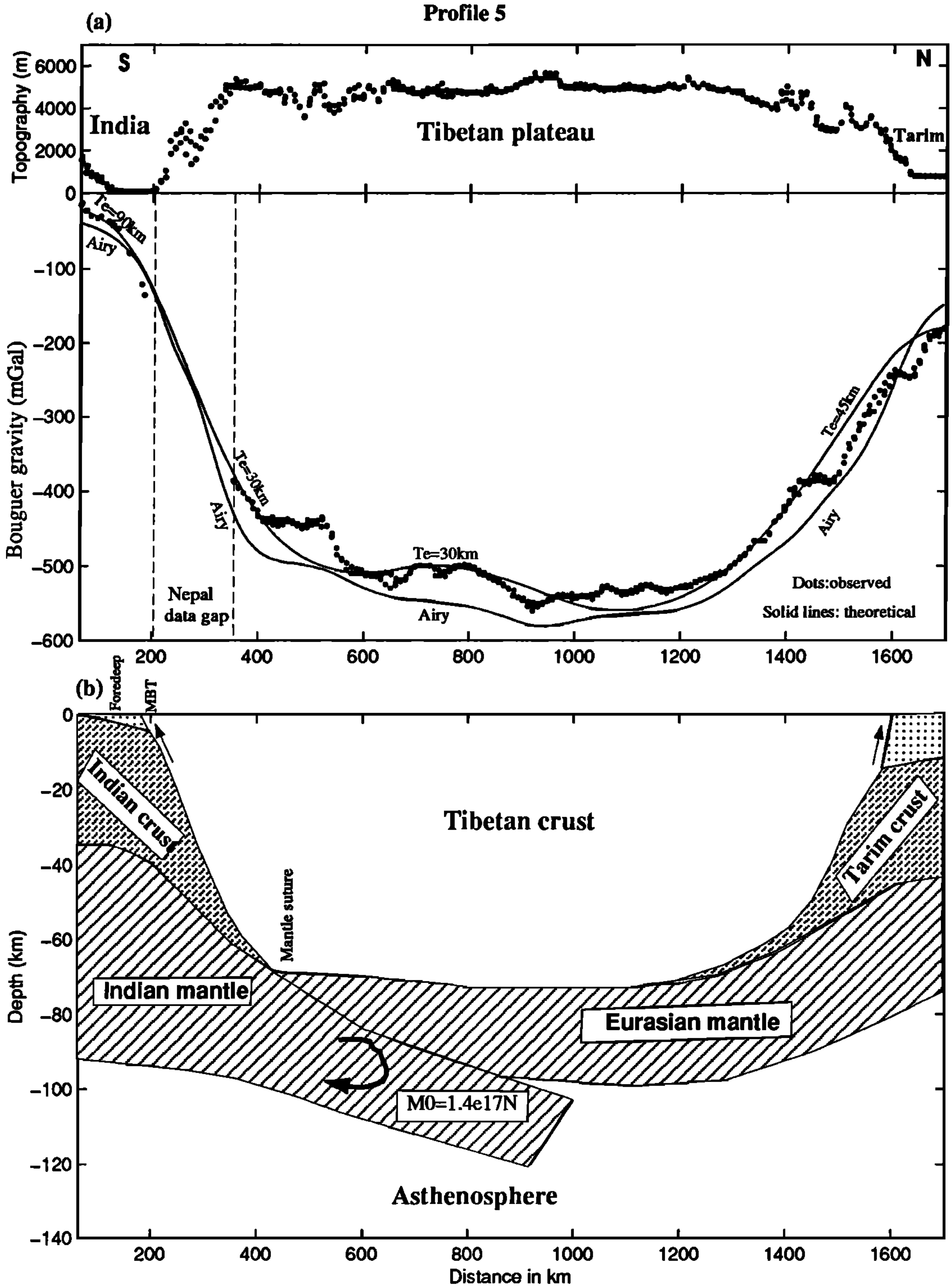

Figure 12. Same as Figure 8, but for profile 5.

proper position (Figure 13) and depth (81 km) to be attributed to stress on this fault. However, the focal mechanism determined for this earthquake is predominantly strike-slip, indicating that motions in the mantle are not quite as simple as our model might suggest.

Other features of our model are not so well supported by other constraints. For example, the oldest core drilled in the Tarim Basin is Ordovician, and the basement may be older than Cambrian based on reflection profiles [*Ma et al.*, 1991]. Thus we are surprised by the 40-km value for Eurasian elastic thickness, a value expected for a continental plate of Mesozoic age. Unexpectedly low values of elastic thickness have elsewhere been attributed to decoupling of the crust and mantle, inelastic failure, or thermal reheating. There is no evidence to date that the crust and the upper mantle are decoupled beneath the Tarim Basin, and from our flexural modeling and the previous work by *Lyon-Caen and Molnar* [1984], we can see that T_e of the Tarim Basin is not greater

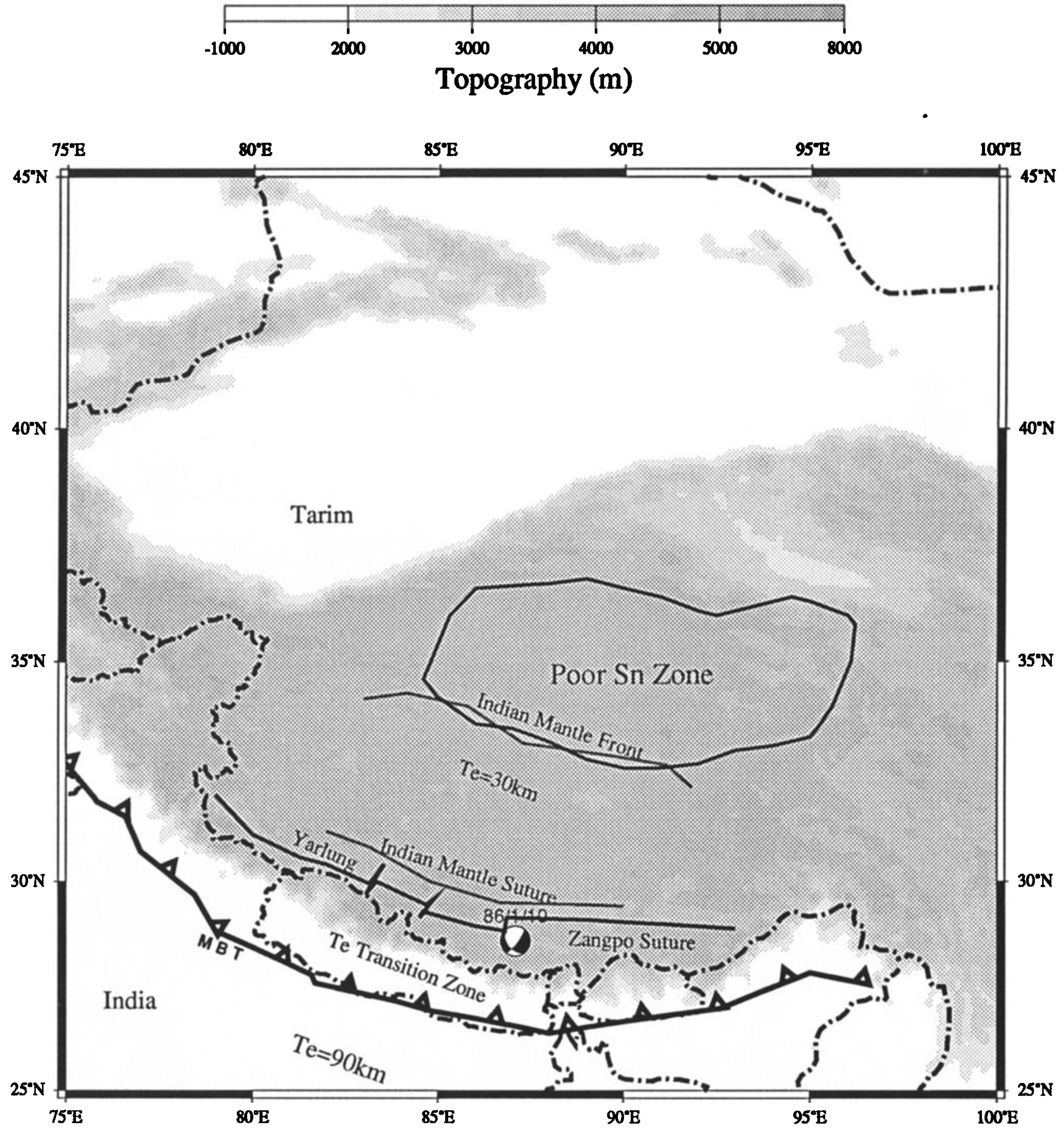

Figure 13. Map view of the locations of the northernmost extent of the Indian plate ("Indian mantle front"), the mantle suture between the Indian and Eurasian plates, and the zone where the Indian plate weakens from T_e=90 km to T_e=30 km based on our flexural modeling. The region of poor propagation of S_n is plotted on the map for comparison. The earthquake focal solution shown is the only one deep earthquake (81 km deep) in the Harvard centroid moment tensor catalogue within the plateau. Its epicenter is close to profile 4 (Figure 1) and its hypocenter is roughly located in the mantle suture zone (Figure 11).

than 45 km even where it is gently flexed before it dives into its southern foredeeps. Thus thermal weakening at the base of the Tarim lithosphere may be a candidate to explain its low T_e value and might contribute to the inefficient propagation of seismic waves noted by *Ni and Barazangi* [1983] beneath the northern plateau. On the other hand, an elastic plate thickness of 45 km is the upper bound found for oceanic lithosphere. Perhaps the Tarim Basin is underlain by oceanic crust [*Hsü*, 1988] which, for some reason, never obtains the elastic strength of continental lithosphere at comparable old ages.

Our model also runs counter to the predictions of many of the theoretical models for the formation of the Tibet plateau, except for those that resemble the model proposed by *Barazangi and Ni* [1982]. For example, our conclusion that the Indian upper mantle is being subducted differs from models that produce distributed shortening and thickening of both Indian and Asian upper mantles beneath Tibet [*Dewey and Bird*, 1970; *Houseman et al.*, 1981]. However, our model also avoids the problem inherent in the distributed shortening models of having to then invoke delamination of the Asian upper mantle through some sort of convection instability [*England and Houseman*, 1989] in order to avoid a thick, cold, dense mantle lid which would be inconsistent with the high elevation of the plateau and the poor propagation of S_n waves beneath north central Tibet.

More recently, *Willett and Beaumont* [1994] have modeled the mantle suture as the junction between a "conveyor belt" (the subducting plate) and a stationary plate (the overriding plate). As the conveyor belt turns, crustal material is transported toward the mantle suture from the descending plate and is scraped off onto the stationary plate on account of decoupling supplied by a weak lower crust. As the crust thickens, the surface suture migrates across the stationary plate away from the mantle suture, such that the former is near one edge of the plateau and the latter is near the other. Therefore, in order to explain the fact that the YZS is near the southern edge of the plateau, *Willett and Beaumont* [1994] must assume that the mantle suture underlies the northern edge of the plateau and that the Eurasian plate is the subducting plate (the conveyor belt). While we agree that a weak lower crust serves to decouple the deformation of the crust from that of the mantle [*Jin et al.*, 1994], we determine the opposite polarity of subduction and a southern position for the mantle suture (Figure 13). Of course, the model of *Willett and Beaumont* [1994] does not yet consider the rheological difference between the plates in the mantle, which indicates that the Eurasian plate is much more easily flexed than the Indian plate, or the effect of isostasy on crustal flow.

The relatively smooth Moho derived from our gravity study does not match the rough, thrusting-dominated structure with a south dipping Moho beneath the High Himalayas and a 20-km-high step near Kangmar as suggested by *Hirn et al.* [1984] and *Hirn* [1988] based on a wide-angle seismic study. Furthermore, *Hirn*'s crustal thickness, about 50 km on average for the Lhasa block and as thin as 40 km in some places, is insufficient for isostatic compensation of the high plateau. This model is also incompatible with *Zhao et al.*'s [1993] smooth, north dipping Moho and J. Ni's [personal communication, 1995] latest broadband results shown in Figure 7. The reason for these discrepancies may be that Hirn's Moho structure is derived from seismic travel times assuming a constant crustal velocity. The seismic refraction data of *Makovsky and Klemperer* [1996] demonstrate that the crustal velocity structure of Tibet is actually quite complicated.

Conclusions

We conclude that it is possible to satisfy the gravity data for Tibet with a very simple, oceanic-type model for plate interactions in the upper mantle in which the mantle portion of a gravitationally heavy Indian plate is subducted beneath the Eurasian plate for a distance of 500-700 km north of the Main Boundary Thrust. The proposal that India is being subducted beneath the southern margin of Asia is certainly not new [*Barazangi and Ni*, 1982; *Argand*, 1924]; however, the Bouguer gravity data have aided in pinpointing the location of the mantle suture and in quantifying the rigidity, depth, and lateral extent of the interacting plates. Our preferred model for the lithospheric structure beneath Tibet includes a stiff (T_e = 90 km but weakening beneath the Himalaya) Indian plate underthrusting Tibet to approximately the YZS subjected to a terminal bending moment supplied by a subducting Indian slab. North of the YZS, the plateau rests upon a moderately stiff (T_e = 40 km) Eurasian plate underthrusting from the north. The elastic plate model is strikingly similar to that originally proposed by *Lyon-Caen and Molnar* [1983]. The fact that the weakening of the Indian plate coincides with the edge of the plateau (Figure 13) suggests that it marks the location where the Indian crust is skimmed off the mantle lithosphere and perhaps injected into the Tibet lower crust in the manner suggested by *Zhao and Morgan* [1987]. Figure 13 also shows the map projection of the mantle suture between the Indian plate and the Eurasian plate; it lies less than 100 km north of YZS, which marks the suture in the upper crust. This model explains 95% of the Bouguer gravity signal, the other 5% apparently arising from folding in the upper crust [*Jin et al.*, 1994].

We determine that the mantle suture between Indian and Asian plates lies just north of the YZS. Over time since the collision, the active surface fault has migrated to the south of the YZS and is now positioned at the MBT (Figure 1). Although our gravity data only provide information on the present geometry of the mantle suture, it is not unreasonable to suggest that the mantle suture has remained relatively stable over the same period if indeed the mantle portion of the plate boundary is behaving in a manner analogous to oceanic subduction. In this case then, the southward migration of the surface suture would not be caused by any fundamental forces in the mantle but rather by the changing state of the stress in the crust caused by the growing gravitational load of the plateau.

When adopting a forward modeling approach, it is impossible to be completely exhaustive in examining models to fit the observations. Nevertheless, we believe that it would be extremely difficult to obtain a comparable fit to the data with models that involve distributed shortening in the upper mantle or subduction of Asia beneath India at a mantle suture beneath the northern plateau.

Of the many surface faults that deform the Tibet crust, only the MBT is directly connected to a fundamental plate boundary in the mantle. Thus we find no evidence for plate tectonic motions in the mantle driving slip along the other faults in the Himalaya and Tibet. *Molnar* [1988] has suggested that the stress induced by the overly thickened crust itself may be what causes the normal faulting in the high Himalaya. Such stresses within the crust may also be responsible for the eastward motion of Tibet [*Dewey et al.*, 1988], given the slightly higher elevation of the plateau in the west.

Acknowledgments. We thank Deborah Hutchinson, Peter Molnar, James Ni, Richard Saltus, and An Yin for useful reviews. This research was supported by NASA (NA65-2928) and NSF (EAR-9304621).

References

Amboldt, N., Relative Schwerkraftsbestimmungen mit Pendeln in Zentral Asien, 2, Reports from Scientific Expedition to Northwestern Province of China under Leadership of Dr. Suen Hedin, *Publ. 30,* II Geodes., Truckeri Akteblaget Tihule, Stockholm, 1948.

Argand, E., La tectonique de l'Asie, Proc. *13th Int. Geol. Congr., 13th,* 171-372, 1924.

Armijo, R., P. Tapponnier, J. L. Mercier, and T. Han, Quaternary extension in southern Tibet: field observations and tectonic implications, *J. Geophys. Res.*, *91*, 13,803-13,872, 1986.

Avouac, J. P., and G. Peltzer, Active tectonics in southern Xinjiang, China: Analysis of terrace riser and normal fault scarp degradation along the Hotan-Qira fault system, *J. Geophys. Res.*, *98*, 21,773-21,807, 1993.

Avouac, J. P., P. Tapponnier, M. Bai, H. You, and G. Wang, Active thrusting and folding along the northern Tien Shan and Late Cenozoic rotation of the Tarim relative to Dzungaria and Kazakhstan, *J. Gephys. Res.*, *98*, 6755-6804, 1993.

Barazangi, M., and J. Ni, Velocities and propagation characteristics of P_n and S_n beneath the Himalayan arc and Tibetan plateau: Possible evidence for underthrusting of Indian continental lithosphere beneath Tibet, *Geology*, *10*, 179-185, 1982.

Beghoul, N., M. Barazangi, and B. L. Isacks, Lithospheric structure of Tibet and western North America: Mechanisms of uplift and a comparative study, *J. Geophys. Res.*, *98*, 1997-2016, 1993.

Boulin, J., Afghanistan structure, Greater India concept and eastern Tethys evolution, *Tectonophysics*, *72*, 261-287, 1981.

Burchfiel, B. C., Q. Deng, P. Molnar, L. Royden, Y. Wang, P. Zhang, and W. Zhang, Intracrustal detachment within zones of continental deformation, *Geology*, *17*, 748-752, 1989.

Dewey, J. F., and P. Bird, Mountain belts and the new global tectonics, *J. Geophys. Res.*, *75*, 2625-2647, 1970.

Dewey, J. F., R. M. Shackleton, C. F. Chang, and Y. Y. Sun, The tectonic evolution of the Tibetan plateau, *Philos. Trans. R. Soc. London A*, *327*, 379-413, 1988.

England, P. C., and D. P. McKenzie, A thin viscous sheet model for continental deformation, *Geophys. J. R. Astron. Soc.*, *70*, 295-321, 1982.

England, P. C., and G. Houseman, Extension during the continental convergence, with application to the Tibet Plateau, *J. Geophys. Res.*, *94*, 17,561-17,579, 1989.

Fielding, E., B. Isacks, M. Barazangi, and C. Duncan, How flat is Tibet?, *Geology*, *22*, 163-167, 1994.

Hirn, A., A. Nercessian, M. Sapin, G. Jobert, Z. X. Xu, E. Y. Gao, D. Y. Lu, and J. W. Teng, Lhasa block and bordering sutures--A continuation of 500-km Moho traverse through Tibet, *Nature*, *307*, 25-27, 1984.

Hirn, A., Features of the crust-mantle structure of Himalayas-Tibet: A comparison with seismic traverses of Alpine, Pyrenean and Variscan orogenic belts, *Philos. Trans. R. Soc. London A*, *326*, 17-32, 1988.

Houseman, G., D. P. McKenzie, and P. Molnar, Convective instability of a thickened boundary layer and its relevance for the thermal evolution of continental convergence belts, *J. Geophys. Res.*, *86*, 6115-6132, 1981.

Hsü, K. J., Relict back-arc basins: Principles of recognition and possible new examples from China, in *Frontiers in Sedimentary Geology: New Perspectives in Basin Analysis*, edited by K. L. Kleinspehn and C. Paolo, pp 245-263, Springer-Verlag, New York, 1988.

Jin, Y., M. K. McNutt, and Y. S. Zhu, Evidence from gravity and topography data for folding of Tibet, *Nature*, *371*, 669-674, 1994.

Karner, G. D., and A. B. Watts, Gravity anomalies and flexure of the lithosphere of mountain ranges, *J. Geophys. Res.*, *88*, 10,449-10,477, 1983.

Kogan, M. G., and M. K. McNutt, Gravity field over northern Eurasia and variations in the strength of the upper mantle, *Science*, *259*, 473-479, 1993.

Lyon-Caen, H., and P. Molnar, Constraints on the structure of the Himalayas from an analysis of gravity anomalies and a flexural model of the lithosphere, *J. Geophys. Res.*, *88*, 8171-8192, 1983.

Lyon-Caen, H., and P. Molnar, Gravity anomalies and the structure of western Tibet and the southern Tarim basin, *Geophys. Res. Lett.*, *11*, 1251-1254, 1984.

Ma, B. L., and Team of Hydrocarbon Geology in Tarim, *Sedimentation and Hydrocarbon in Tarim*, Sci. Publ., Beijing, 1991.

Makovsky, Y., and S. L. Klemperer, Structural elements of the southern Tethyan Himalaya crust from wide-angle seismic data, *Tectonics*, in press, 1996.

Masek, J. G., B. L. Isacks, and E. J. Fielding, Rift flank uplift in Tibet: Evidence for a viscous lower crust, *Tectonics*, *13*, 659-667, 1994.

McAdoo, D. C., and D. T. Sandwell, Folding of oceanic lithosphere, *J. Geophys. Res.*, *90*, 8563-8569, 1985.

McNamara, D. E., T. J. Owens, P. G. Silver, and F. T. Wu, Shear wave anisotropy beneath the Tibetan plateau, *J. Geophys. Res.*, *99*, 13,655-13,665, 1994.

McNamara, D. E., T. J. Owens, and W. R. Walter, Observations of regional phase propagation across the Tibetan plateau, *J. Geophys. Res.*, *100*, 22,215-22,229, 1995.

Molnar, P., A review of geophysical constraints on the deep structure of the Tibetan plateau, the Himalayas and the Karakorum, and their tectonics, *Philos. Trans. R. Soc. London A*, *326*, 33-88, 1988.

Molnar, P., and H. Lyon-Caen, Fault plane solutions of earthquakes and active tectonics of Tibetan plateau and its margins, *Geophys. J. Int.*, *99*, 123-153, 1989.

Molnar, P., and P. Tapponnier, Cenozoic tectonics of Asia: Effects of a continental collision, *Science*, *189*, 419-426, 1975.

Ni, J., and M. Barazangi, High frequency seismic wave propagation beneath the Indian shield, Himalayan arc, Tibetan plateau and surrounding regions: High uppermost mantle velocities and inefficient propagation beneath Tibet, *Geophys. J. R. Astron. Soc.*, *72*, 665-689, 1983.

Okabe, M., Analytical expressions for gravity anomalies due to homogeneous polyhedral bodies and translations into magnetic anomalies, *Geophysics*, *44*, 730-741, 1979.

Pan, Y., and W. S. F. Kidd, Nyainqentanglha shear zone: A late Miocene extensional detachment in the southern Tibetan Plateau, *Geology*, *20*, 775-778, 1992.

Royden, L. H., The tectonic expression of slab pull at continental convergent boundaries, *Tectonics*, *12*, 303-325, 1993.

Royden, L., and B. C. Burchfiel, Crustal thickening in eastern Tibet without surface shortening: A natural result of flow within a weak lower crust, *EOS Trans. AGU*, *76*, Fall Meet. Suppl., F567, 1995.

Sheffels, B., and M. McNutt, Role of subsurface loads and regional compensation in the isostatic balance of the Transverse Ranges, California: Evidence for intracontinental subduction, *J. Geophys. Res.*, *91*, 6419-6431, 1986.

Sinha-Roy, S., Introductions of Tethyan blocks and evolution of Asian fold belt, *Tectonophysics*, *82*, 277-297, 1982.

Smith, R. B., Formation of folds, boudinage, and mullions in non-Newtonian materials, *Geol. Soc. Am. Bull.*, *88*, 312-320, 1977.

Sun, W., Bouguer gravity anomaly map of the People's Republic of China, Chin. Acad. of Geoexplor., Beijing, 1989.

Tapponnier, P., G. Peltzer, and A. Y. Ledain, Extrusion tectonics in Asia: New insights from simple experiments with plasticine, *Geology*, *10*, 611-616, 1982.

Teng, J. W., and Tarim Geophysics Group, *The geophysical field and hydrocarbon in the Tarim Basin*, pp. 20 and 60, Sci. Publ., Beijing 1991.

Watts, A. B., G. D. Karner, P. Wessel, and J. Hastings, Global gravity bank system, *Tech. Rep. 4, CU-1-85*, Off. of Nav. Res., Washington, D.C., 1985.

Willett, S. D., and C. Beaumount, Subduction of Asian lithospheric mantle beneath Tibet inferred from models of continental collision, *Nature*, *369*, 642-645, 1994.

Wu, G. J., X. C. Xiao and T. D. Li, *Yadong to Golmud Transect: Qinghai-Tibetan Plateau, China*, Global Geosci. Transects, Vol. 3, AGU, Washington, D. C., 1991.

Yin, A., T. M. Harrison, F. J. Ryerson, W. Chen, W. S. F. Kidd, and P. Copeland, Tertiary structural evolution of the Gangdese thrust system, southeastern Tibet, *J. Geophys. Res.*, *99*, 18,175-18,201, 1994.

Zhao, W. J., K. D. Nelson, and Project INDEPTH Team, Deep seismic reflection evidence for continental underthrusting beneath southern Tibet, *Nature*, *366*, 557-559, 1993.

Zhao, W. L., and J. Morgan, Injection of Indian crust into Tibetan lower crust: A two-dimensional finite element model study, *Tectonics*, *6*, 489-504, 1987.

Y. Jin and M. K. McNutt, Department of Earth, Atmospheric, and Planetary Sciences, Massachusetts Institute of Technology, Cambridge, MA 02139. (e-mail: jin@bullard.mit.edu; marcia@mit.edu)

Y. Zhu, Department of Marine Geology, Ocean University of Qingdao, 266003 Qingdao, People's Republic of China.

(Received July 14, 1995; revised January 30, 1996; accepted February 6, 1996.)